Rate Retardation Trends in RAFT - An Emerging Monomer

**Classification Tool?** 

Tochukwu Nwoko<sup>a</sup>, Khoi Nguyen<sup>a</sup>, Nirob K. Saha, Christopher Barner-Kowollik, Dominik

Konkolewicza, \*

\*Correspondence: d.konkolewicz@miamiOH.edu

<sup>a</sup> Department of Chemistry and Biochemistry, Miami University, 651 E High St. Oxford, OH,

45056, USA

<sup>b</sup> Centre for Materials Science, School of Chemistry and Physics, Queensland University of

Technology (QUT), 2 George Street, Brisbane, Queensland 4000, Australia

**Abstract** 

Rate retardation is a common and unusual feature of reversible addition-fragmentation chain-

transfer (RAFT) polymerization, where a decline in polymerization rate occurs with higher

concentrations of the chain transfer agent (CTA). The strength of retardation depends on the RAFT

equilibrium constant between the RAFT intermediate radical and the propagating radical plus

CTA. Rate retardation occurs for both the more activated monomers (MAMs) and the less activated

monomers (LAMs). Herein, we exploit the ubiquitous phenomenon of RAFT rate retardation to

identify the unique RAFT kinetics of MAMs: methyl methacrylate, styrene, phenyl vinyl ketone,

methyl acrylate, and dimethyl acrylamide, as well as LAMs: vinyl acetate and N-vinyl pyrrolidone.

Investigating the above monomers indicates that LAMs and acrylic/acrylamide monomers show substantial retardation, even using optimized conditions targeting polymers of over a degree of polymerization near 1000. In contrast, highly activated monomers such as styrene, methyl methacrylate, and phenyl vinyl ketone showed only weak retardation under their optimized conditions at near a target degree of polymerization of 300. The analysis indicates that even within the MAM family, there exist differences in monomer reactivity, with acrylic/acrylamide monomers having lower reactivity and higher propensity for retardation, than methacrylic, vinyl ketone, or styrene monomers. The current study highlights how retardation kinetics in RAFT be used to extract general trends in monomer reactivity and radical stabilization that can be employed to preplan polymerization outcomes.

# Introduction

Polymers are ubiquitous,<sup>1</sup> and with increased emphasis on efficient use of resources, there is a significant drive towards the development of new and efficient polymerization techniques.<sup>2–5</sup> Conventional free radical polymerization (FRP) presents a platform for polymer synthesis from a large pool of vinyl monomers under mild reaction conditions.<sup>6</sup> In addition to the homopolymerization of monomers, FRP allows copolymerization of distinct monomers, thus introducing complex polymer functionalities into the resulting polymer structures.<sup>7</sup> Due to its simplicity and tolerance to functional groups, FRP is essential in industry, with polymers that are typically made by FRP such as low-density polyethylene (LDPE), polyvinyl chloride (PVC), polystyrene (PSty) representing close to ~40% of the polymer volume produced.<sup>8</sup> However, the FRP involves highly reactive radicals that propagate for a very short time in the order of 1 s, followed by irreversible chain termination or transfer. These irreversible chain stoppage events in

FRP limit the control over the polymer in terms of the degree of polymerization, end group functionality, molecular weight distribution, and polymer microstructure/segmentation.<sup>9</sup>

Reversible deactivation radical polymerization (RDRP) techniques combine the living characteristics of ionic polymerization with the versatility of a conventional radical polymerization process. 10–12 RDRP methods allow the facile synthesis of structurally complex polymers 13 such as block, branched, and star polymers, while controlling composition, topology, end-group fidelity<sup>14</sup>, and the chain length distribution of the synthesized polymers. 4,15,16 Control in RDRP processes critically depends on a dynamic equilibrium between active radicals and dormant species.<sup>17</sup> Reversible addition-fragmentation chain-transfer (RAFT) polymerization is one of the most common RDRP techniques. 14,18 RAFT polymerization can be performed under mild reaction conditions and provides excellent control over polymer architecture for a wide variety of vinyl monomers. 16 In the RAFT process, the radicals are generated either thermally or photochemically and react with monomers, yielding a propagating radical species. Control in RAFT polymerization is obtained through a chain transfer agent (CTA).<sup>19</sup> The propagating radicals add to the CTA and entering a preequilibrium stage entailing a RAFT intermediate radical. The intermediate radical fragments, yielding a leaving group radical and a dormant polymer chain (macroCTA).<sup>20</sup> As the small molecule CTA is converted to macroCTA, the system progressively enters the main equilibrium. In the RAFT main equilibrium, a propagating polymeric radical adds to a polymeric CTA, 21,22 generating a RAFT intermediate radical. The RAFT intermediate radical can undergo subsequent fragmentation allowing the efficient exchange of chains between dormant/macroCTA states and active/propagating radical states. The equilibrium and exchange dynamics provides near uniform growth of the polymers, <sup>23,24</sup> as demonstrated in Scheme 1. As in all radical polymerization processes, every radical that is present in the reaction system is potentially able to terminate with

other radicals, with electronic and steric effects dictating the radical's propensity to undergo disproportionation and combination processes. In the RAFT process, this implies that the RAFT intermediate radical can - in both the pre- and main equilibrium - potentially also undergo termination events.

# Initiation Radical Source $\xrightarrow{k_d}$ $I^{\bullet}$ $I^{\bullet} + M \longrightarrow P_m^{\bullet}$ Pre Equilibrium $P_m^{\bullet} + \sum_{Z} S_{R} \xrightarrow{k_{add}} P_m \xrightarrow{S_{Z}} S_{R} \xrightarrow{k_{\beta}} P_m \xrightarrow{S_{Z}} S_{R} \xrightarrow{k_{\beta}} P_m \xrightarrow{S_{Z}} S_{R} \xrightarrow{k_{\alpha}} P_m \xrightarrow{S_{\alpha}} S_{R} \xrightarrow{k_{\beta}} P_m \xrightarrow{S_{\alpha}} S_{R} \xrightarrow{k_{\alpha}} P_m \xrightarrow{k_{\alpha}} S_{R} \xrightarrow{k_{\alpha}} S_{R$

Scheme 1: Mechanism of RAFT polymerization and (pre and main equilibrium and also IRT and SFM models)

The RAFT CTA is a thiocarbonylthio compound, Z-C(=S)-S-R, in the majority of cases. The choice of CTA is governed by the type of vinyl monomers to be polymerized. For the efficient deactivation of propagating radicals, the C=S bond should be more reactive towards radical addition than the C=C bond of the vinyl monomer. The reactivity of the C=S bond to radical addition and the stability of the intermediate radical is controlled by the Z group of the CTA.<sup>20</sup> The

more activated monomers (MAMs) require a Z group that strongly stabilizes the subsequent intermediate radical, while the less activated monomers (LAMs) require relatively less stable intermediate radicals<sup>20,21</sup> to favor the fragmentation of the propagating radical. The leaving group, R, should be chosen such that the intermediate radical fragments towards the leaving group over the monomer derived radical, and the R radical should readily add to the monomer for efficient initialization of the polymerization.

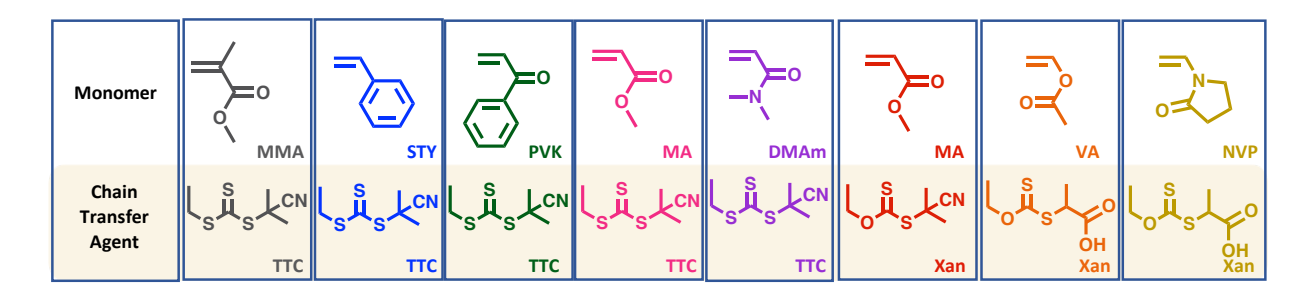
Ideally, the RAFT process uses a CTA to control the relative chain length of polymer chains without interfering with the polymerization rate, <sup>20,25</sup> since the addition and fragmentation rates ideally yield a low and constant intermediate radical concentration. However, rate retardation has been observed in RAFT polymerizations, 21,22,26 where decreases in the polymerization rate occur with higher CTA concentrations. A wide range of models<sup>27–32</sup> have been proposed to explain rate retardation, some of them featuring significant complexity. Yet, on a fundamental level, rate retardation can be explained by two basic models. On the one hand, Barner-Kowollik et al. suggested the phenomenon to be caused by slow fragmentation of the intermediate radical(s),<sup>33</sup> while deBouwer et al. proposed the possibility of the cross termination of intermediate radicals with propagating radicals.<sup>34</sup> These two mechanisms of retardation are captured within Scheme 1. In addition, there are other less complex causes of rate retardation, which can be avoided by careful experimentation, including impurities or oxygen interference, as well as a poor choice of CTA, e.g., a non-initiating R-group. A carefully matched CTA-monomer system ensures good control of polymerization, however a common feature in all RAFT polymerizations is the formation of the intermediate radical. Since retardation is tied to the intermediate radical, retardation is tied to control in RAFT polymerizations.<sup>22</sup>

The dithiobenzoates CTA family has an aromatic phenyl-moiety attached as the Z group. The aromatic ring ensures relatively higher stabilization of the intermediate radical by allowing for delocalization of the unpaired electron<sup>34</sup> and inducing slower fragmentation.<sup>22</sup> In prior work,<sup>22</sup> rate retardation was investigated in systems beyond the traditional dithiobenzoate CTAs. Methyl methacrylate (MMA), methyl acrylate (MA), styrene (STY), and vinyl acetate (VA) were matched with optimal CTAs<sup>20</sup> as defined in the literature and subjected to series of experiment with steadily increasing CTA concentration. These systems<sup>22</sup> displayed rate retardation irrespective of monomer class. However, the choice of an optimized CTA for each monomer, which often varied between monomers, limited direct comparison of reactivity between the wide variety of monomers that RAFT is compatible with. The current contribution investigates rate retardation in systems spanning from MAMs to LAMs with only two classes of CTA, i.e., trithiocarbonates (TTC) for MAMs and xanthates (Xan) for LAMs, as well as one acrylic monomer. Retardation rates were explored for each monomer-CTA pair, highlighting trends in activity. Both the SFM and the IRT models have each been adapted to a simple scaling law analysis that is a function of the RAFT equilibrium constant.<sup>26</sup> Combining systematic kinetic experiments across a range of monomers with an IRT and SFM scaling laws analysis allows the RAFT equilibrium constant to be extracted  $(K_{RAFT})$ , enabling the evaluation of each monomer's reactivity in RAFT. This analysis suggests the existence of clusters of LAMs, but also MAMs with substantially weaker and stronger retardation, and thereby reactivity.

# **Results and Discussion**

A series of RAFT polymerization were performed for the most commonly polymerized RAFT monomers, i.e., the MAMs MMA, MA, STY, *N,N*-dimethyl acrylamide (DMAm), and

phenyl vinyl ketone (PVK), as well as the LAMs of VA and *N*-vinylpyrrolidone (NVP). For the polymerization of the MAMs (MMA, STY, PVK, MA, DMAm), the CTA 2-cyanoprop-2-yl ethyl trithiocarbonate (CPETC) was employed, allowing the direct comparison between all MAMs. Additionally, MA was studied with both CPETC and cyano-isopropyl ethyl xanthate (CIPEX) in order to evaluate the impact of using the less active xanthate CTA in CIPEX relative to the more active trithiocarbonate in CPETC. This difference in activity between CTAs is due to trithiocarbonate CTA having a more stabilizing Z group (*S*-alkyl) relative to the xanthate (Z= *O*-alkyl) CTA.<sup>20</sup> Further, the LAMs (VA, NVP) were all polymerized using 2-(ethoxycarbonothioyl) sulfanyl propanoic acid (EtPAX) as the xanthate CTA. An overview of all explored monomers and CTAs is provided in Scheme 2.



**Scheme 2:** Monomer and matching CTA systems explored in the current study.

To elucidate the retardation effects, for each monomer-CTA pair only the concentration of the CTA is altered, while the temperature and concentrations of AIBN, monomer, and solvent remain constant. Through this experimental design, changes in polymerization rate must be attributed to RAFT retardation effects, as all other experimental variables remain constant. However, by keeping the concentration of AIBN constant with changes in CTA concentration, the ratio of AIBN:CTA necessarily changes across the experiment, with higher target molecular weight experiments having higher AIBN:CTA ratios. Literature reported temperatures were either

unchanged or slightly modified in each polymerization system. The temperature for MA,<sup>22</sup> DMAM,<sup>35</sup> PVK and NVP<sup>36</sup> was set to 60 °C, 65 °C for styrene,<sup>37</sup> 70 °C for MMA, and 55 °C for VA<sup>22</sup>.

One of the most polymerized monomer families is the acrylates. <sup>20,38</sup> Both trithiocarbonate and xanthate CTAs were employed in MA polymerization to highlight the influence of control on the severity of rate retardation in a commonly studied monomer. The vinyl group of MA is conjugated with a carbonyl group that will yield relatively more stabilized radicals. The trithiocarbonate CTAs due to their more stabilizing Z group (S-alkyl) offer better control during the polymerization of MA relative to the xanthates (Z=O-alkyl) CTAs.<sup>20</sup> Figure 1A and 1B depict kinetic data for the polymerization of MA in DMSO at 60 °C mediated by CPETC or CIPEX. In these experiments the MA:AIBN ratio was maintained at 100:0.2, with varying amounts of CTAs in both systems. A gradual decrease in polymerization rate was visible in both systems at higher CTA concentrations, which is indicative of rate retardation.<sup>22</sup> As expected, retardation was stronger for the more active trithiocarbonate CTA and less significant for the less active xanthate CTA, evidenced by similar or even faster steady state polymerization rates for MA polymerization, targeting chain length close to 33 using CiPEX as the CTA or approximately 100 using CPETC as the CTA. Induction periods, especially at higher CTA loading, may be due to the slow addition of the more stabilized tertiary cyanoisopropyl radical to the secondary MA monomer. However, other factors such as SFM and IRT mechanisms during the pre-equilibrium may also contribute to these induction periods. Figures 1 C depicts good correlation of experimental  $M_n$  and theoretical  $M_n$  ( $M_{n-1}$ ) <sub>th</sub>) for systems with higher CEPTC concentration and low dispersity  $(M_w/M_n)$  in the order of 1.1-1.3. When using the less active CIPEX CTA, the dispersities is substantially higher, ranging from 1.4 to 1.9, although the correlation of  $M_n$  with  $M_{n-th}$  remains acceptable, in agreement with

literature-reported trends when comparing high and low activity CTAs in the same monomeric system. <sup>25,39–41</sup> These data also suggest there can be a tradeoff between polymerization rate, which increases with lower activity CTAs, and the uniformity of chains, which decreases with lower activity CTAs<sup>25</sup>. <sup>25</sup>

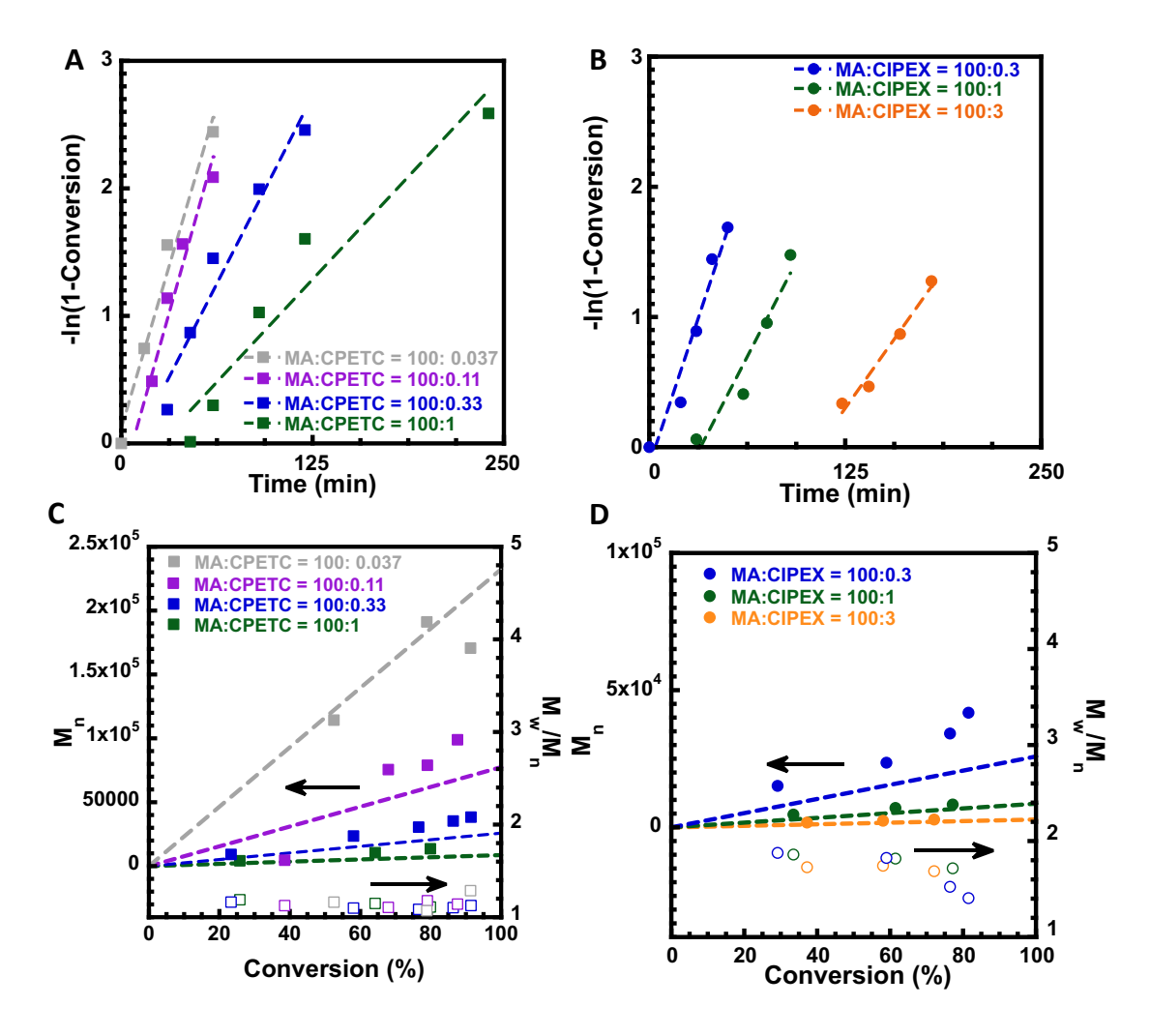


**Figure 1.** Kinetic data for RAFT polymerization of MA.(A) MA polymerization kinetics with CPETC (B) MA polymerization kinetics with CIPEX. (C) Evolution of  $M_n$  (solid point)  $M_{n-th}$  (dashed line) and  $M_w/M_n$  (hollow points) with CPETC (D) Evolution of  $M_n$  (solid point)  $M_{n-th}$  (dashed line) and  $M_w/M_n$  (hollow points) with CIPEX Reactions were run at 60 °C with [MA]:[AIBN] = 100:0.2 and MA:CTA ratios given in the legend at 50% MA in DMSO.

Figure 2 shows the polymerization kinetics of the acrylic more active monomers of DMAm (A), MA (B), and MMA (C), polymerized by RAFT using CPETC to mediate the polymerization process. A clear difference in results is observed for each of these monomers. Both DMAm and

MA display strong retardation effects, requiring targeted chain lengths of close to 3000 and 1000 to show minimal impact of CTA concentration on the reaction rate. This is evidenced by the DMAm polymerization with a targeted chain length of approx. 9000, featuring a similar polymerization rate to that of targeted chain length of ~3000. When targeting very high molecular weight DMAm polymers of 3000 or higher, the viscosity was very high at conversions near 50%, making sampling at high conversion difficult. Similarly, during MA polymerization, the rate at a targeted chain length of ~3000 is similar to the polymerization rate of targeted chain length of ~1000. Further, comparing MMA to MA, the effect of radical stability is apparent. MMA generates a tertiary resonance stabilized radical, which should be more stable than the secondary radicals resonance stabilized generated in the polymerization of DMAm and MA. The radical stability difference is reflected in the extent of retardation, with MMA having similar polymerization rates at targeted chain lengths of ~3000, 1000, and 300. Only when reaching targeted chain length of 100 do retardation effects become apparent.

Figure S1 gives the evolution of  $M_n$  and  $M_{n-th}$  vs Conversion and  $M_w/M_n$  values for DMAm polymerization with CPETC, while Figure S2 gives the evolution for  $M_n$  and  $M_{n-th}$  vs Conversion and  $M_w/M_n$  values for MMA polymerization with CPETC. The control over molecular weight and dispersity was notably better for MA and DMAm polymerization compared to MMA. Indeed, dithiobenzoates are generally considered better CTAs for methacrylate, although acceptable control can be achieved with CPETC. These results comparing DMAm, MA and MMA are qualitatively consistent with those comparing MA with different CTAs, notably that systems with stronger retardation effects often lead to better-controlled polymers.

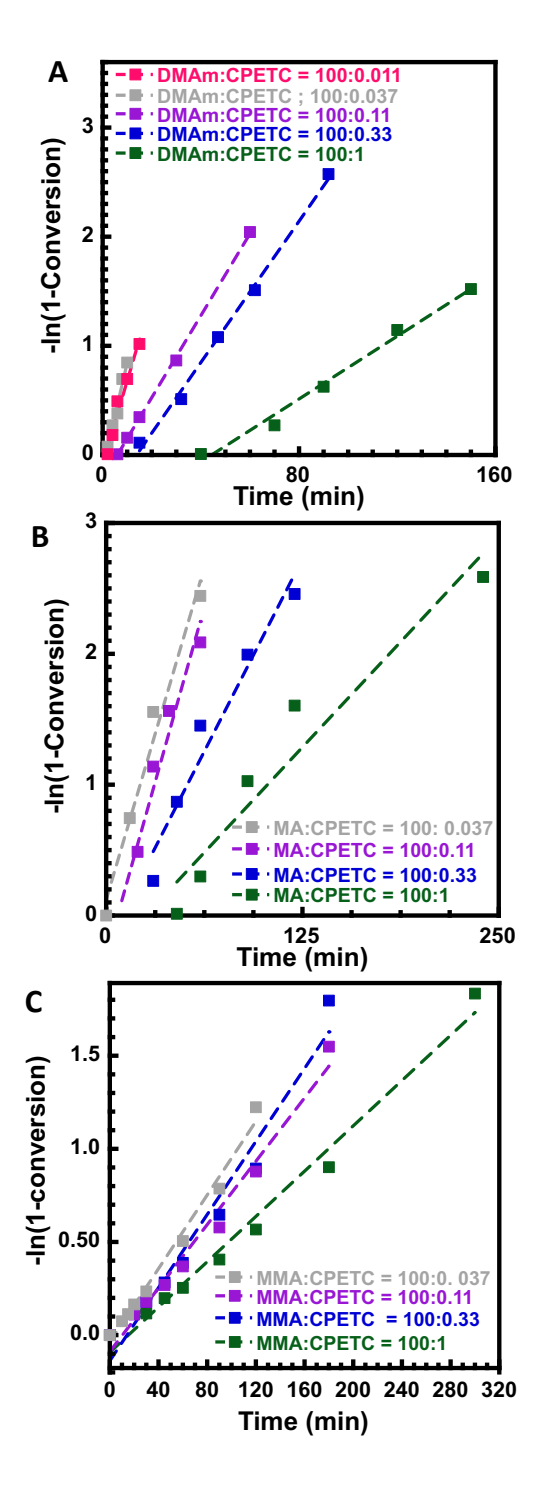


**Figure 2.** Kinetic data for RAFT polymerization (A) DMAm polymerization kinetics with CPETC at 60 °C with [DMAm]:[AIBN] = 100:0.2 and DMAm:CPETC ratios given in the legend at 50 % DMAm in DMSO (B) MA polymerization kinetics with CPETC at 60 °C with [MA]:[AIBN] = 100:0.2 and MA:CPETC ratios given in the captions at 50 % MA in DMSO (C) MMA

polymerization kinetics with CPETC at 70 °C with [MMA]:[AIBN] = 100:0.2 and MMA:CPETC ratios given in the captions at 50% MMA in DMSO.

However, there remain monomers in the MAM family that are not acrylic in nature. Both styrene and vinyl ketone polymers can be efficiently polymerized by RAFT. As seen in Figure 3, these 3 polymerizations are subject to substantially less retardation effects than the acrylic monomers of MA and DMAm when using trithiocarbonate CTAs. To record measurable retardation, STY had to reach a targeted chain length of close to 100 units to show even very mild retardation effects, while PVK showed minimal evidence of retardation, even towards a targeted chain length of approx. 10 monomers, after an induction period in both cases. Indeed, there is no evidence of reduction of slope of the semilogarithmic plot in the polymerization of PVK, although there is an increase in induction period for PVK at higher chain lengths. All slopes are within 13% of the mean for the PVK systems.

Comparable to MMA, which only showed retardation effects near a targeted chain length of around 100 units. Overall, these data indicate that STY, PVK, and MMA behave differently to MA and DMAm, with substantially less retardation than the acrylic monomers. Interestingly, the PVK and STY polymers synthesized by RAFT have good agreement between  $M_n$  and  $M_{n-th}$  and overall low dispersities, as seen in Figure S3 and S4 respectively. The STY and PVK data indicate that although molecular weight uniformity and retardation are often correlated, this is not true in all cases. This is likely correlated with the fact that control over molecular weight distribution is a kinetic phenomenon related  $^{42-45}$  to the ratio of propagation to RAFT exchange rates, while retardation is tied to the RAFT equilibrium constant ( $K_{RAFT}$ ). It is possible for a polymerization reaction to feature a high rate of exchange, even if it has a small  $K_{RAFT}$ , if the rates of fragmentation and addition are comparable and both high.

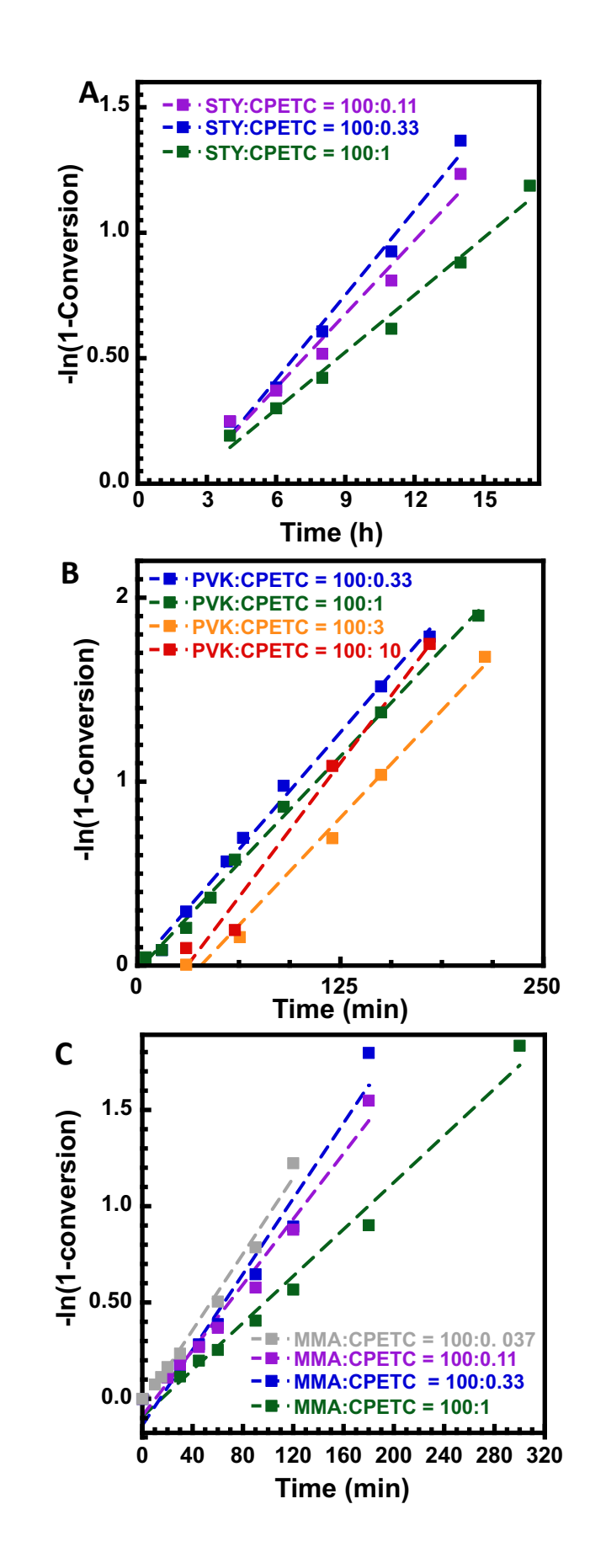
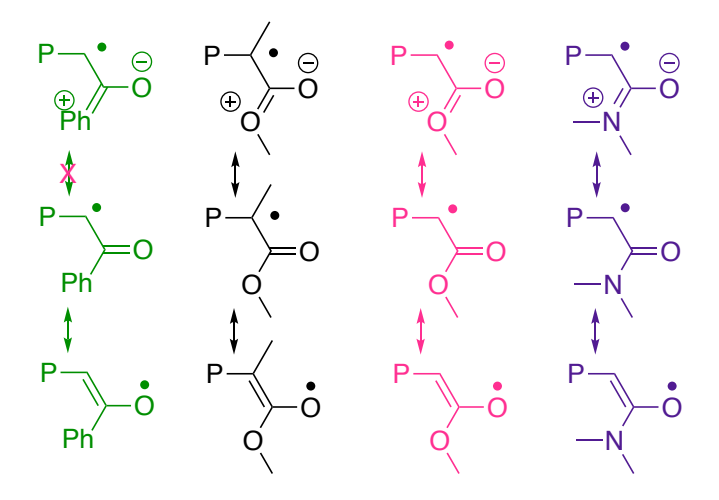


**Figure 3.** Kinetic data for RAFT polymerization (A) STY polymerization kinetics with CPETC at 65 °C with [STY]:[AIBN] = 100:0.2 and STY:CPETC ratios given in the captions in bulk (B) PVK polymerization kinetics with CPETC at 60 °C with [PVK]:[AIBN] = 100:0.067 and PVK:CPETC ratios given in the legend at 33 % PVK in DMSO (C) MMA polymerization kinetics with CPETC at 70 °C with [MMA]:[AIBN] = 100:0.2 and MMA:CPETC ratios given in the captions at 50% MMA in DMSO.

A possible reason for the observed trend in retardation for the acrylic monomers and the vinyl ketone is the strength of resonance delocalization. As seen in Scheme 3, the acrylic propagating radicals all have contributions from donation of the lone pair on the acrylic ester methoxy group or dimethyl amino group. However, this is not possible for PVK due to the phenyl group not having a lone pair, as the lone pair into the ester/amide of MMA, MA, or DMAm. The lone pair reduces the  $\pi$ -bond character of the resonance stabilizing C=O group. Due to the lower  $\pi$ -bond characteristic, the acrylic radicals from MMA, MA, and DMAm should be less stabilized by resonance than PVK type analogues. Further, the dimethyl amino groups are better at electron-donation than methoxy groups, as measured by the Hammett parameter, <sup>46</sup> which explain why the extent of retardation is stronger for DMAm than MA. Therefore, the tertiary and secondary radical stability can be used to rationalize the small extent of retardation in MMA compared to MA.



Scheme 3: Resonance structures for propagating radicals from left to right of PVK, MMA, MA, and DMAm.

Finally, LAM monomers of NVP and VA were polymerized using EtPAX as the CTA. As evidenced in Figure 4, retardation was strong for both VA and NVP, requiring targeted chain lengths of close to 900 for NVP and 300 for VA to see retardation effects. Despite the less reactive xanthate CTA used in the polymerization of NVP and VA, the low radical stabilization led to strong retardation effects, due to no resonance delocalization of the unpaired electron in the propagating radical. Interestingly, a similar effect is seen when comparing DMAm vs MA, and NVP vs VA. In both cases, the amide-containing monomer led to stronger retardation effects than the ester-containing monomer, plausibly due to the effects of stronger lone pair donation in nitrogen-reducing radical stability.

As indicated in Figure S5 and S6, the evolution of  $M_n$  with conversion is linear with relatively low dispersity for lower targeted chain length (100 and 300). The dispersity and control over the polymerization were poor at longer chain lengths for VA and NVP polymerization. For NVP polymerization, the correlation of  $M_n$  with  $M_{n-th}$  was relatively poor, presumably due to the use of PMMA calibrants for poly (NVP) molecular weight analysis in SEC. The limited control over molecular weight at higher targeted chain lengths for VA and NVP polymerization is most likely

due to side reactions such as chain transfer reactions that can be prevalent in the polymerization with these highly reactive radicals.

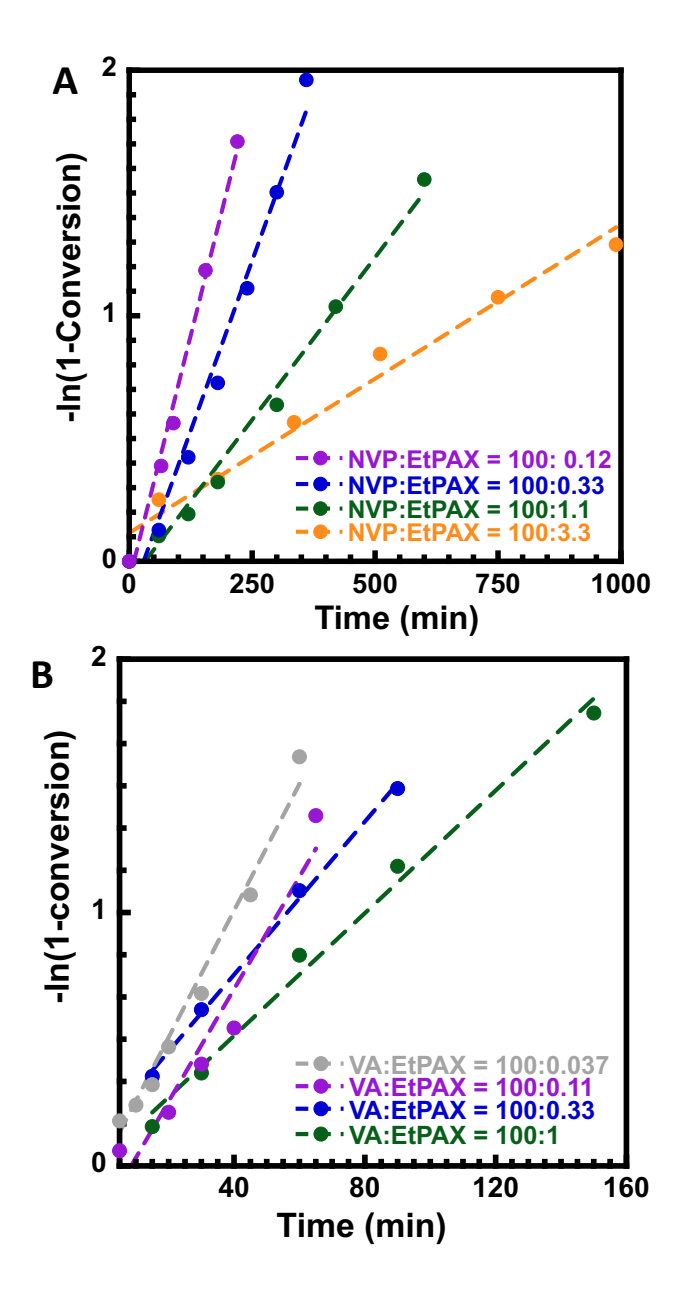


**Figure 4.** Kinetic data for RAFT polymerization (A) NVP polymerization kinetics with EtPAX at 60 °C with [NVP]:[AIBN] = 100:0.56 and NVP:EtPAX ratios given in the captions at 40% NVP in dioxane (B) VA polymerization kinetics with EtPAX at 55 °C with [VA]:[AIBN] = 100:0.5 and VA:EtPAX ratios given in the legend at 50 % VA in DMSO.

Since the kinetic experiments in Figures 1-4 focused on determining concentrations of CTA where RAFT retardation is either dominant and concentrations where retardation is minor, the earlier derived scaling laws for IRT and SFM models of RAFT retardation<sup>22</sup> can be applied to the wide range of monomers studied here. It is important to note that the current study applies both models indiscriminately without exploring their different advantages and disadvantages, which have been explored in substantial details elsewhere,<sup>47</sup> including in our most recent contribution.<sup>22</sup> Finally, the current contribution will not explore the intermediate models that have been proposed to describe all available experimental data coherently, such as the one proposed by Konkolewicz *et al.* in 2009.<sup>48</sup> An analysis based on these highly parameterized models is challenging and, perhaps most importantly, will not allow to arrive at different conclusions in terms of establishing a taxonomy of globally observed rate retardation effects during RAFT polymerization. The next section will briefly reiterate the applied scaling laws and the assumptions underpinning them.<sup>22</sup>

Assuming the rate of cross-termination and conventional termination are similar,  $^{49,50}$  the propagating radical concentration [P $^{\bullet}$ ] in the IRT model can be related to the propagating radical concentration under ideal free radical polymerization conditions [P $^{\bullet}$ ]<sub>0</sub> as follows:<sup>22</sup>

$$\frac{[P\cdot]}{[P^{\cdot}]_{0}} = \frac{1}{(1+K_{RAFT}[CTA])^{1/2}} \tag{1}$$

Where here  $K_{RAFT}$  is the RAFT equilibrium constant and [CTA] is the concentration of CTA used in that experiment. Similarly, for the SFM, the ratio of radical concentration under RAFT conditions to ideal free radical polymerization conditions is given by:<sup>22</sup>

$$\frac{[P]}{[P]_0} = tanh\left(\frac{[P]_0 k_t t}{K_{RAFT}[CTA]}\right) \tag{2}$$

Where tanh is the hyperbolic tangent function,  $k_t$  is the conventional termination rate coefficient, t is the reaction time, and  $K_{RAFT}$  and [CTA] have the same meaning as in Eq 1. It is important to

note that since the SFM is not a steady state model, each time point must be individually analyzed in the SFM. In contrast, in the IRT the steady state assumption allows the fitting of a line to the semilogarithmic kinetic plot, to give an apparent rate of propagation,  $k_p^{app}$ , which is related to [P $^{\bullet}$ ] as follows:

$$k_p^{app} = k_p[P] \tag{3}$$

Where  $k_p$  is the propagation rate coefficient. Finally  $[P^{\bullet}]_0$  can be estimated by applying the steady state approximation to radical generation from AIBN and conventional termination in a standard free radical process as follows:

$$[P^{\cdot}]_{0} = \sqrt{\frac{2fk_{d}[AIBN]}{k_{t}}} \tag{4}$$

Where f is the initiator efficiency,  $k_d$  is the dissociation rate coefficient of the radical initiator AIBN, and  $k_t$  is the conventional radical termination rate coefficient. Using eq 1-4, and a fitting process for SFM outlined in the supporting information values for  $K_{RAFT}$  could be fitted for all polymerization studied in Figures 1-4. Limited literature data exists for  $K_{RAFT}$  values for trithiocarbonate or xanthate CTAs, since much of the prior studies have focused on dithiobenzoates where retardation effects are exceptionally strong.<sup>31</sup>

Figure 5A shows that the IRT model provides a prima-facie excellent description of all 8 polymerization systems with vastly different monomers. However, it should be noted that this simplified version of the IRT model cannot capture the inhibition periods explicitly, but instead fits the steady state rate after any induction periods. The strength of retardation in the IRT model is governed by the product of  $K_{RAFT}$  and [CTA]. The IRT analysis highlights two regimes. When

 $K_{\text{RAFT}} \times [\text{CTA}]$  is substantially less than 1, retardation is almost absent, whereas when  $K_{\text{RAFT}} \times$ [CTA] is substantially greater than 1, the radical concentration scales with a -0.5 order in both  $K_{RAFT}$  and [CTA], leading to a strong retardation. In RAFT polymerization, the typical targeted chain length is close 100 units, and using monomer concentrations between 1 and 5 M indicates that a typical CTA concentration is on the order of 10 to 50 mM for a RAFT reaction. Since the transition from weakly to strongly retarded RAFT processes occurs when  $K_{RAFT} \times [CTA] \sim 1$ , using a 40 mM CTA concentration gives  $K_{RAFT} \sim 40 \text{ M}^{-1}$  as an approximate value of  $K_{RAFT}$  at the onset of retardation (assuming targeted DP 100). With this in mind, inspection of Figure 5A and Table 1 suggests that 3 monomers fall into the weakly retarded regime, which are MMA, STY, and PVK when using trithiocarbonate CTAs. Unsurprisingly, these monomers are all MAMs. However, two other MAMs, MA and DMAm, have K<sub>RAFT</sub> values in the order of 100 or above with the trithiocarbonate CTA that is well suited for their polymerization. Indeed, when using a xanthate with MA, the RAFT equilibrium constant falls below 100, but narrow molecular weight distributions were not observed (Figure 1). Additionally, the LAMs of VA and NVP also fall into a strongly retarded regime with  $K_{RAFT} > 100$  in both cases, even when using the low-activity xanthate CTA.

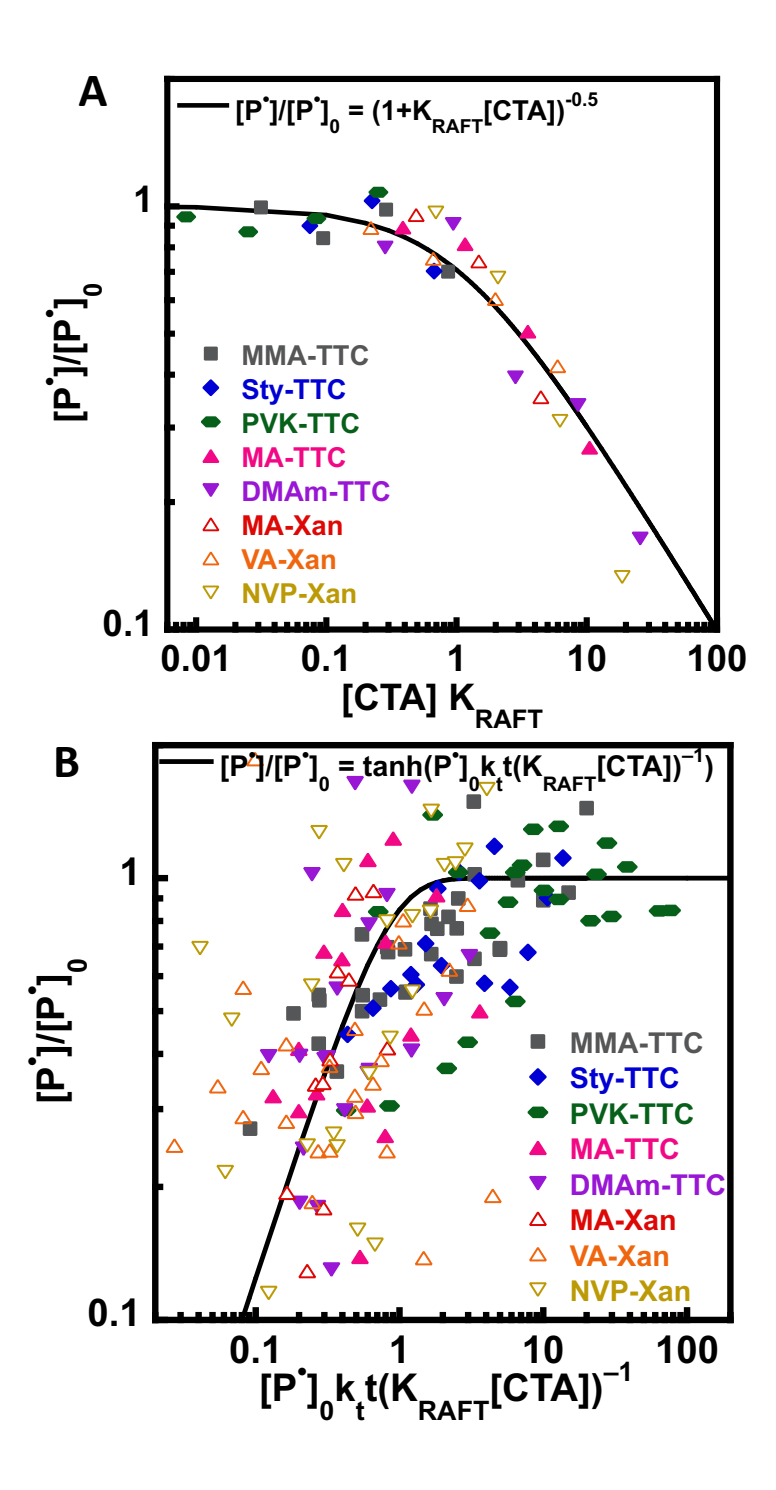


Figure 5. (A) IRT scaling analysis propagating radical concentration ([P $^{\bullet}$ ]) compared to that of the ideal free radical polymerization ([P $^{\bullet}$ ] $_0$ ) across all 8 monomer-CTA pairs studied with fitted  $K_{RAFT}$ .

(B) SFM scaling analysis propagating radical concentration ([P $^{\bullet}$ ]) compared to that of the ideal free radical polymerization ([P $^{\bullet}$ ] $_0$ ) across all 8 monomer-CTA pairs studied with fitted  $K_{RAFT}$ .

SFM analysis is given in Figure 5B. Due to the non-steady state nature of the SFM, each individual timepoint must be analyzed separately, leading to a substantial increase in the observed data scatter, as the SFM-derived data are not the results of a fitting exercise over a set of many data points, as is possible in the IRT model. Therefore, in the SFM analysis performed at this level of the model, induction periods due to the build-up of RAFT intermediate radical cannot be decoupled from induction periods due to transitions from RAFT pre-equilibrium to the main equilibrium, which can somewhat lower the quality of fit to the kinetic data. In general, the SFM captures the general trends in RAFT retardation well. However, due to the noted factors regarding not available global fitting and – at this level of model simplicity – not differentiating between the pre- and mainequilibrium, the fit is less clear. Nevertheless, the trends in K<sub>RAFT</sub> again suggest that PVK and MMA are among the least retarded monomers, however, induction periods then lead to an overestimation of  $K_{RAFT}$  for STY. Other monomer-CTA combinations with an estimated  $K_{RAFT}$  >  $10^6 \,\mathrm{M}^{-1}$  are indicative of strong retardation, except for MA with the xanthate, which has a  $K_{\mathrm{RAFT}}$ of just under  $10^6$  M<sup>-1</sup>. The values of  $K_{RAFT}$  for the slow fragmentation model in Table 1 are within an order of magnitude of values reported in earlier work for both styrene and methyl acrylate with trithiocarbonate CTAs, and vinyl acetate with a xanthate CTA.  $^{22}$  Additionally, the estimated  $K_{RAFT}$ IRT value for MA with the trithiocarbonate CTA at 60 °C is within an order of magnitude of the K<sub>RAFT</sub> measured for butyl acrylate with a trithiocarbonate CTA at 70 °C determined by EPR. The different temperatures do not allow direct comparison however.<sup>51</sup>

**Table 1.** Estimated  $K_{RAFT}$  values for all polymerizations studied in both IRT and SFM analysis for both trithiocarbonate (TTC) and Xanthate (Xan) CTAs.

Monomer	CTA Type	Kraft-irt (M <sup>-1</sup> )	Kraft-sfm (M <sup>-1</sup> )
MMA	TTC	1.8×10 <sup>1</sup>	5.4×10 <sup>5</sup>

Sty	TTC	7.7×10 <sup>0</sup>	2.0×10 <sup>6</sup>
PVK	TTC	$1.0 \times 10^{0}$	$2.3 \times 10^4$
DMAm	TTC	$5.3 \times 10^2$	$2.0 \times 10^6$
MA	TTC	$1.9 \times 10^{2}$	$2.0 \times 10^6$
MA	Xan	$8.0 \times 10^{1}$	$9.1 \times 10^5$
VA	Xan	$1.1 \times 10^2$	$9.9 \times 10^{5}$
NVP	Xan	$5.0 \times 10^2$	1.8×10 <sup>6</sup>

Overall, the analysis suggests that RAFT retardation falls into two main classes of monomer. MMA, PVK, and STY have very low extents of retardation with trithiocarbonate CTAs and as a result, they are well described as MAMs. Lower activity monomers of VA and NVP, which are well described as LAMs, showing strong retardation, even with the low activity xanthate CTA. Finally, acrylic monomers such as MA and DMAm have reasonably strong retardation with trithiocarbonate CTAs, but MA shows poor control with xanthate CTAs. Therefore, these monomers are still MAMs from the perspective that trithiocarbonate CTAs are needed for control, however, their stronger retardation rates infer lower activity than other MAMs, such as PVK, STY, and MMA. Thus, RAFT rate retardation and its scaling analysis can be used to highlight trends in monomer reactivity.

### Conclusion

Surprisingly, RAFT polymerization is subject to rate retardation, where a consistent decline in polymerization rate is observed with increasing CTA concentrations. The effect of retardation across 7 monomers and 8 distinct pairs of monomer/CTA combinations highlights the trends in retardation across the commonly polymerized classes of monomers. In particular, retardation analysis shows how MAMs of methyl methacrylate, phenyl vinyl ketone, and styrene have

relatively low retardation, with the vinyl ketone monomer having the least retardation. LAMs of vinyl acetate and N-vinyl pyrrolidone have strong retardation, even with xanthate CTAs. Finally, acrylic monomers of methyl acrylate and N,N-dimethylacrylamide have moderate-to-strong retardation with trithiocarbonate CTAs, while methyl acrylate has much weaker retardation with a xanthate CTA. Scaling analysis via the intermediate termination model and slow fragmentation model allows estimation of RAFT equilibrium constants, in turn allowing renormalization and subsequent collapse of all kinetic data onto a single function. The kinetic and scaling analysis suggests that the extent of retardation can be employed as a tool to investigate monomer reactivity trends. Further, it opens the door to the polymerization of MAMs with stronger stabilization of the propagating radical and lower retardation, as well as MAMs of weaker stabilization of the propagating radical and stronger retardation, in addition to the LAMs which exhibit strong retardation.

# Acknowledgements

D.K. acknowledges support from the National Science Foundation under award number CHE-2203727 for polymer synthesis and kinetic experiments and IRT analysis. C.B.-K. acknowledges the Australian Research Council (ARC) for a Laureate Fellowship and the Queensland University of Technology (QUT) for continued support.

### Reference

- (1) Zhang, K.; Monteiro, M. J.; Jia, Z. Stable Organic Radical Polymers: Synthesis and Applications. *Polym Chem* **2016**, *7* (36), 5589–5614.
- (2) Zhang, Y.; Dubé, M. A. Green Emulsion Polymerization Technology. *Polymer Reaction Engineering of Dispersed Systems: Volume I* **2018**, 65–100.

- (3) Scholten, P. B. V; Moatsou, D.; Detrembleur, C.; Meier, M. A. R. Progress toward Sustainable Reversible Deactivation Radical Polymerization. *Macromol Rapid Commun* **2020**, *41* (16), 2000266.
- (4) Bhattacharjee, M.; Pramanik, N. B.; Singha, N. K.; Haloi, D. J. Recent Advances in RDRP-Modified Chitosan: A Review of Its Synthesis, Properties and Applications. *Polym Chem* **2020**, *11* (42), 6718–6738.
- (5) Parnitzke, B.; Nwoko, T.; Bradford, K. G. E.; Watuthanthrige, N. D. A.; Yehl, K.; Boyer, C.; Konkolewicz, D. Photons and Photocatalysts as Limiting Reagents for PET-RAFT Photopolymerization. *Chemical Engineering Journal* **2023**, *456*, 141007.
- (6) Matyjaszewski, K.; Davis, T. P. Handbook of Radical Polymerization. 2002.
- (7) Fukuda, T.; Kubo, K.; Ma, Y.-D. Kinetics of Free Radical Copolymerization. *Prog Polym Sci* **1992**, *17* (5), 875–916.
- (8) Geyer, R.; Jambeck, J. R.; Law, K. L. Production, Use, and Fate of All Plastics Ever Made. *Sci Adv* **2017**, *3* (7), e1700782.
- (9) Krys, P.; Matyjaszewski, K. Kinetics of Atom Transfer Radical Polymerization. *Eur Polym J* **2017**, *89*, 482–523.
- (10) Braunecker, W. A.; Matyjaszewski, K. Controlled/Living Radical Polymerization: Features, Developments, and Perspectives. *Prog Polym Sci* **2007**, *32* (1), 93–146.
- (11) Parkatzidis, K.; Wang, H. S.; Truong, N. P.; Anastasaki, A. Recent Developments and Future Challenges in Controlled Radical Polymerization: A 2020 Update. *Chem* **2020**, *6* (7), 1575–1588.
- (12) Truong, N. P.; Jones, G. R.; Bradford, K. G. E.; Konkolewicz, D.; Anastasaki, A. A Comparison of RAFT and ATRP Methods for Controlled Radical Polymerization. *Nat Rev Chem* **2021**, *5* (12), 859–869.
- (13) Destarac, M. Industrial Development of Reversible-Deactivation Radical Polymerization: Is the Induction Period Over? *Polym Chem* **2018**, *9* (40), 4947–4967.
- (14) Truong, N. P.; Jones, G. R.; Bradford, K. G. E.; Konkolewicz, D.; Anastasaki, A. A Comparison of RAFT and ATRP Methods for Controlled Radical Polymerization. *Nat Rev Chem* **2021**, *5* (12), 859–869. https://doi.org/10.1038/s41570-021-00328-8.
- (15) Corrigan, N.; Jung, K.; Moad, G.; Hawker, C. J.; Matyjaszewski, K.; Boyer, C. Reversible-Deactivation Radical Polymerization (Controlled/Living Radical Polymerization): From Discovery to Materials Design and Applications. *Prog Polym Sci* **2020**, *111*, 101311.
- (16) Tsarevsky, N. V; Matyjaszewski, K. "Green" Atom Transfer Radical Polymerization: From Process Design to Preparation of Well-Defined Environmentally Friendly Polymeric Materials. *Chem Rev* **2007**, *107* (6), 2270–2299.
- (17) Matyjaszewski, K. The Importance of Exchange Reactions in Controlled/Living Radical Polymerization in the Presence of Alkoxyamines and Transition Metals. In *Macromolecular symposia*; Wiley Online Library, 1996; Vol. 111, pp 47–61.
- (18) Parkatzidis, K.; Wang, H. S.; Truong, N. P.; Anastasaki, A. Recent Developments and Future Challenges in Controlled Radical Polymerization: A 2020 Update. *Chem* **2020**, *6* (7), 1575–1588.
- (19) Sun, M.; Szczepaniak, G.; Dadashi-Silab, S.; Lin, T.; Kowalewski, T.; Matyjaszewski, K. Cu-Catalyzed Atom Transfer Radical Polymerization: The Effect of Cocatalysts. *Macromol Chem Phys* **2023**, *224* (3), 2200347.

- (20) Perrier, S. 50th Anniversary Perspective: RAFT Polymerization ☐ A User Guide. *Macromolecules* **2017**, *50* (19), 7433–7447.
- (21) Barner-Kowollik, C.; Buback, M.; Charleux, B.; Coote, M. L.; Drache, M.; Fukuda, T.; Goto, A.; Klumperman, B.; Lowe, A. B.; Mcleary, J. B. Mechanism and Kinetics of Dithiobenzoate-mediated RAFT Polymerization. I. The Current Situation. *J Polym Sci A Polym Chem* **2006**, *44* (20), 5809–5831.
- (22) Bradford, K. G. E.; Petit, L. M.; Whitfield, R.; Anastasaki, A.; Barner-Kowollik, C.; Konkolewicz, D. Ubiquitous Nature of Rate Retardation in Reversible Addition—Fragmentation Chain Transfer Polymerization. *J Am Chem Soc* **2021**, *143* (42), 17769—17777.
- (23) Matyjaszewski, K. Macromolecular Engineering: From Rational Design through Precise Macromolecular Synthesis and Processing to Targeted Macroscopic Material Properties. *Prog Polym Sci* **2005**, *30* (8–9), 858–875.
- (24) Matyjaszewski, K.; Tsarevsky, N. V. Macromolecular Engineering by Atom Transfer Radical Polymerization. *J Am Chem Soc* **2014**, *136* (18), 6513–6533.
- (25) Nwoko, T.; Watuthanthrige, N. D. A.; Parnitzke, B.; Yehl, K.; Konkolewicz, D. Tuning the Molecular Weight Distributions of Vinylketone-Based Polymers Using RAFT Photopolymerization and UV Photodegradation. *Polym Chem* **2021**, *12* (46), 6761–6770.
- (26) Monteiro, M. J.; de Brouwer, H. Intermediate Radical Termination as the Mechanism for Retardation in Reversible Addition—Fragmentation Chain Transfer Polymerization. *Macromolecules* **2001**, *34* (3), 349–352.
- Vana, P.; Davis, T. P.; Barner-Kowollik, C. Kinetic Analysis of Reversible Addition Fragmentation Chain Transfer (RAFT) Polymerizations: Conditions for Inhibition, Retardation, and Optimum Living Polymerization. *Macromol Theory Simul* **2002**, *11* (8), 823–835.
- (28) Moad, G. Mechanism and Kinetics of Dithiobenzoate-Mediated RAFT Polymerization—Status of the Dilemma. *Macromol Chem Phys* **2014**, *215* (1), 9–26.
- (29) Moad, G. Mechanism and Kinetics of Dithiobenzoate-Mediated RAFT Polymerization—Status of the Dilemma. *Macromol Chem Phys* **2014**, *215* (1), 9–26.
- (30) Kwak, Y.; Goto, A.; Fukuda, T. Rate Retardation in Reversible Addition—Fragmentation Chain Transfer (RAFT) Polymerization: Further Evidence for Cross-Termination Producing 3-Arm Star Chain. *Macromolecules* **2004**, *37* (4), 1219–1225.
- (31) Barner-Kowollik, C.; Buback, M.; Charleux, B.; Coote, M. L.; Drache, M.; Fukuda, T.; Goto, A.; Klumperman, B.; Lowe, A. B.; Mcleary, J. B. Mechanism and Kinetics of Dithiobenzoate-mediated RAFT Polymerization. I. The Current Situation. *J Polym Sci A Polym Chem* **2006**, *44* (20), 5809–5831.
- (32) Chernikova, E.; Golubev, V.; Filippov, A.; Lin, C. Y.; Coote, M. L. Use of Spin Traps to Measure the Addition and Fragmentation Rate Coefficients of Small Molecule RAFT-Adduct Radicals. *Polym Chem* **2010**, *1* (9), 1437–1440.
- (33) Keddie, D. J.; Moad, G.; Rizzardo, E.; Thang, S. H. RAFT Agent Design and Synthesis. *Macromolecules* **2012**, *45* (13), 5321–5342.
- (34) Ranieri, K.; Delaittre, G.; Barner-Kowollik, C.; Junkers, T. Direct Access to Dithiobenzoate RAFT Agent Fragmentation Rate Coefficients by ESR Spin-Trapping. *Macromol Rapid Commun* **2014**, *35* (23), 2023–2028.
- (35) Gibson, R. R.; Fernyhough, A.; Musa, O. M.; Armes, S. P. RAFT Dispersion Polymerization of N, N-Dimethylacrylamide in a Series of n-Alkanes Using a

- Thermoresponsive Poly (Tert-Octyl Acrylamide) Steric Stabilizer. *Polym Chem* **2021**, *12* (14), 2165–2174.
- (36) Mishra, V.; Kumar, R. RAFT Polymerization of N-vinyl Pyrrolidone Using Prop-2-ynyl Morpholine-4-carbodithioate as a New Chain Transfer Agent. *J Appl Polym Sci* **2012**, *124* (6), 4475–4485.
- (37) Arita, T.; Buback, M.; Janssen, O.; Vana, P. RAFT-Polymerization of Styrene up to High Pressure: Rate Enhancement and Improved Control. *Macromol Rapid Commun* **2004**, *25* (15), 1376–1381.
- (38) Martin, L.; Gody, G.; Perrier, S. Preparation of Complex Multiblock Copolymers via Aqueous RAFT Polymerization at Room Temperature. *Polym Chem* **2015**, *6* (27), 4875–4886.
- (39) Whitfield, R.; Parkatzidis, K.; Truong, N. P.; Junkers, T.; Anastasaki, A. Tailoring Polymer Dispersity by RAFT Polymerization: A Versatile Approach. *Chem* **2020**, *6* (6), 1340–1352.
- (40) Parkatzidis, K.; Truong, N. P.; Antonopoulou, M. N.; Whitfield, R.; Konkolewicz, D.; Anastasaki, A. Tailoring Polymer Dispersity by Mixing Chain Transfer Agents in PET-RAFT Polymerization. *Polym Chem* **2020**, *11* (31), 4968–4972.
- (41) Whitfield, R.; Truong, N. P.; Anastasaki, A. Precise Control of Both Dispersity and Molecular Weight Distribution Shape by Polymer Blending. *Angewandte Chemie* **2021**, *133* (35), 19532–19537.
- (42) Konkolewicz, D.; Siauw, M.; Gray-Weale, A.; Hawkett, B. S.; Perrier, S. Obtaining Kinetic Information from the Chain-Length Distribution of Polymers Produced by RAFT. *J Phys Chem B* **2009**, *113* (20), 7086–7094.
- (43) Kearns, M. M.; Morley, C. N.; Parkatzidis, K.; Whitfield, R.; Sponza, A. D.; Chakma, P.; Watuthanthrige, N. D. A.; Chiu, M.; Anastasaki, A.; Konkolewicz, D. A General Model for the Ideal Chain Length Distributions of Polymers Made with Reversible Deactivation. *Polym Chem* **2022**, *13* (7), 898–913.
- (44) Goto, A.; Fukuda, T. Kinetics of Living Radical Polymerization. *Prog Polym Sci* **2004**, *29* (4), 329–385.
- (45) Harrisson, S. The Chain Length Distribution of an Ideal Reversible Deactivation Radical Polymerization. *Polymers (Basel)* **2018**, *10* (8), 887.
- (46) Hansch, C.; Leo, A.; Taft, R. W. A Survey of Hammett Substituent Constants and Resonance and Field Parameters. *Chem Rev* **1991**, *91* (2), 165–195.
- (47) Barner-Kowollik, C.; Buback, M.; Charleux, B.; Coote, M. L.; Drache, M.; Fukuda, T.; Goto, A.; Klumperman, B.; Lowe, A. B.; Mcleary, J. B. Mechanism and Kinetics of Dithiobenzoate-mediated RAFT Polymerization. I. The Current Situation. *J Polym Sci A Polym Chem* **2006**, *44* (20), 5809–5831.
- (48) Konkolewicz, D.; Hawkett, B. S.; Gray-Weale, A.; Perrier, S. RAFT Polymerization Kinetics: How Long Are the Cross-terminating Oligomers? *J Polym Sci A Polym Chem* **2009**, *47* (14), 3455–3466.
- (49) Kwak, Y.; Goto, A.; Fukuda, T. Rate Retardation in Reversible Addition—Fragmentation Chain Transfer (RAFT) Polymerization: Further Evidence for Cross-Termination Producing 3-Arm Star Chain. *Macromolecules* **2004**, *37* (4), 1219–1225.
- (50) Barner-Kowollik, C.; Buback, M.; Charleux, B.; Coote, M. L.; Drache, M.; Fukuda, T.; Goto, A.; Klumperman, B.; Lowe, A. B.; Mcleary, J. B. Mechanism and Kinetics of Dithiobenzoate-mediated RAFT Polymerization. I. The Current Situation. J Polym Sci A Polym Chem 2006, 44 (20), 5809–5831.

(51) Meiser, W.; Barth, J.; Buback, M.; Kattner, H.; Vana, P. EPR Measurement of Fragmentation Kinetics in Dithiobenzoate-Mediated RAFT Polymerization. *Macromolecules* **2011**, *44* (8), 2474–2480. https://doi.org/10.1021/ma102491x.